Influence of blended powders on properties of Ultra-High Strength Fibre Reinforced Self Compacting Concrete subjected to elevated temperatures

Mohamed S. Saif [a,*], Ali S. Shanour [a], Gamal E. Abdelaziz [a], Hanaa I. Elsayad [a], Ibrahim G. Shaaban [b], Bassam A. Tayeh [d], Mahmoud S. Hammad [c]

[a] *Department of Civil Engineering, (Shoubra), Benha University, 108 shoubra street, 11629 Cairo, Egypt*
[b] *School of Computing and Engineering,University of West London, UK*
[c] *Department of Civil Engineering, Beni Suef University, Egypt*
[d] *Civil Engineering Department, Faculty of Engineering, Islamic University of Gaza, Palestine*

ARTICLE INFO

ABSTRACT

Ultra-High Strength Fibre Reinforced Self Compacting Concrete (UHSFRSCC) is in great demand for use in construction projects around the globe. Unless fillers are utilised in this concrete, its production will come at an excessive environmental cost due to the high Carbon footprint of Portland cement. A gap in the published literature was identified, where quaternary mixes, containing Portland cement with three fillers, incorporating fibres, and achieving ultra high strength, were not cited. In this study ternary and quaternary mixes were designed and produced, satisfying the European Guidelines for SCC, with compressive strengths exceeding 115 MPa. Some mixes had compressive strengths between 125 and 150 MPa, which were not previously reported in the literature. The mixes contained Silica Fume (SF), Metakaolin (MK), Limestone powder (LS) as partial Portland cement replacement and quartz powder (QP) as partial sand replacement. Basalt Fibres were added to reinforce the matrix. Compressive & tensile strength of the mixes along with UPV, sorptivity, absorption and SEM Micro-structure features were studied at ambient temperature and after the samples were exposed to either 200 or 300 °C; since the behaviour of HSC at elevated temperature is always a cause for concern. The active and inert fillers exhibited a synergic behaviour at all temperature conditions. The mix containing: 15 % SF, 5 % MK, 20 % LS and 34 % QP achieved the best performance. Compressive and splitting tensile strength improve by 10 % and 17 % while sorptivity and absorption decline by 40 % and 29 % respectively at ambient temperature. Residual compressive strength improved by 10 % and 19 % while, residual splitting tensile strength significantly increases by 21 % and 28 % after exposure to elevated

temperatures 200 ℃ and 300 ℃ respectively. Meanwhile, residual sorptivity decreases by 39 % and 38 % after exposure to these elevated temperatures. Microstructure properties supported and agreed with the mechanical and permeation characteristics results. The results will contribute to the development of UHSFRSCC in hot weather countries.

1. Introduction

Self-compacting concrete or self-consolidating concrete (SCC) is a concrete which possess the following properties: low yield stress, high deformability, good segregation resistance and moderate viscosity [1]. SCC was developed in Japan in 1988, as durable concrete, which can fill every corner of formwork even with congested reinforcement, regardless of the skill of the workers on site. At the time, Japan was facing shortages of experienced labour in the construction industry [2]. In mix design, SCC is considered as a particle suspension, where the coarse aggregate is regarded as the solid phase suspended in the continuous phase micro- or fine mortar [3]. Essentially, SCC is produced by limiting the maximum size and content of coarse aggregates, inclusion of active or inert fillers [4–6] and utilising special workability and viscosity modifying admixtures [7]. High strength (50–100 MPa) and ultra high strength (100–150 MPa) SCC has been used in many mega projects around the world, especially in high-rise buildings, marine facilities, and long span bridges [8–10]. With the high strength comes two concerns: brittleness and behaviour at elevated temperatures [11,12]. To induce more ductility fibres are extensively used in the production of high strength SCC [13–18]. These include steel, polypropylene and Basalt fibres. As for the elevated temperature behaviour, both fibres and fillers were found to be helpful in that respect, as shall be discussed in the following sections.

In a comprehensive review, Salari et al. [18] analysed publications on high strength fibre reinforced SCC between 2005 and 2016. They noted that amongst the commonly used fibres in high strength SCC are Basalt Fibres. Basalt Fibres are environment friendly as they are produced by smelting volcanic rocks in a non-hazardous manner, with less energy consumption than the process for making glass fibres. Hence these fibres are less expensive than carbon fibres and glass fibres [19]. Basalt fibres have superior properties including bond behaviour, mechanical strength (tensile strength approximately 4800 MPa), excellent acoustic/electrical/thermal properties, moderate density (lower than steel fibres but higher than glass fibres), explosion resistance, and capability of combating high pH values [20]. Several investigators have successfully produced SCC or normal concrete with Basalt fibres [19,21–26]. Others reported some decrease in compressive strength, especially at high volumes of additions, but an enhancement of tensile and flexural strengths, with the inclusion of Basalt Fibres [27–30]. Amongst the benefits of this fibre is its ability to improve the behaviour of different types of concrete at elevated temperatures (polymer concrete [31], concrete with recycled aggregates [23,32], high strength concrete [25], and concrete containing stone powder [30]. However, as with all fibres, the workability of concrete is adversely affected by fibre introduction and hence the content in SCC should be limited [19,29,33].

In SCC, Portland cement needs to be partially replaced by active or inert fillers to avoid excessive shrinkage / heat of hydration and to reduce costs [34,35]. The active fillers include pozzolanic materials such as Silica Fume (SF) and Metakaolin (MK), whereas the inert fillers include Quartz Powder (QP) and Limestone Powder (LS). Both types of fillers play positive roles in hydration process, with inert fillers affecting the rate of hydration at early ages (up to 7 days), whereas active fillers contributing to the formation of additional hydration products (after 28 days) [36]. As there is increased societal pressures towards sustainable development, resource efficiency and working towards a more circular economy [37,38], utilisation of fillers in SCC can be helpful in reducing the Carbon footprint as seen in Table 1.

SF has been successfully used in the production of SCC and reactive powder concrete (RPC) [41–43]. MK has also gained wide recognition as a suitable filler in SCC and RPC [43–47]. SF, MK, and LS were found to improve bleeding and segregation resistance in fresh SCC; reduce absorption and enhance the compressive strength of hardened SCC and RPC [43,48–52]. QP was found to reduce the water demand and improve the flow in SCC mixes with SF [53]. The short-term degrees of hydration in mortars containing QP were found to be higher than those for a reference mortar [54]. However, when QP replaced Portland cement, some reduction in strength was reported [35,55], therefore in the current investigation QP was employed as sand replacement to improve the packing density of the mixture. Pastes with LS was found to be more cohesive (higher viscosity) at a given superplasticizer dosage and hence the LS pastes were more segregation resistant [56]. Data from Corinaldesi and Moriconi [57] showed that LS improved the fresh properties of SCC. LS greatly increased the stability and homogeneity of SCC [58]. LS was found to act as an accelerator during early cement hydration [59]. Because of these benefits European and North American standards now allow 5–35 % of LS to be blended in commercial cements, depending on its type and application [60].

A number of investigators studied the effect of fillers on the behaviour of concrete after exposure to elevated temperatures [31,32,

Table 1
Global warming potential of Portland cement and fillers.

Material	GWP (kg CO$_2$/kg)
Portland Cement (OPC)	0.951 [39]
Silica fume (SF)	0.028 [39]
Metakaolin (MK)	0.175 [40]
Limestone Powder (LS)	0.0172 [39]
Quartz Powder (QP)	0.0234 [39]

61,62]. It has been established that SF improves the physico-mechanical properties as well as the microstructure after heating to 600 °C [63]. For example, the replacement of Portland cement with 10 %, 20 %, or 30 % SF by weight improved the compressive strength by 64.6 %, 28 % or 28 % at 600 °C, respectively, compared to the control mix without silica fume [64]. Concrete samples, containing 0 %, 6 %, or 9 % MK, which were heated for two hours at 300 °C, showed 7 %, 16 %, or 14 % increase in compressive strength, respectively [65]. MK, SF and Fly Ash, with replacement ratios of up to 15 %, showed excellent temperature resistance after exposure to up to 900 °C [62]. A mortar blend with 10 % SF and 10 % MK exhibited superior performance after exposure to 800 °C [66]. Mixes with up to 30 %LS, without polypropylene fibres, exhibited a smaller reduction in strength after exposure to 200 °C, compared to their counterparts with polypropylene fibres for all replacement ratios [67]. Partial replacement of cement with up to 20 % QP was reported to improve the thermal and shock resistance after exposure to various temperatures of up to 1000 °C for 2 h [68].

2. Research significance

When combining active fillers with inert fillers, the fillers act in a co-operative manner, exhibiting what is called synergic effect [69]. This is why SCC mixes are usually binary (i.e. containing Portland cement and one filler [58,70–74], ternary (i.e. containing Portland cement and two fillers [70–72,75–80], or quaternary (i.e. containing Portland cement and three fillers [37,72,75,76,81–87]. In the published literature, binary and ternary blends were sometimes reported to achieve strengths between 110 and 180 MPa [65,69, 73,79,80,88], with or without added fibres. However, the compressive strength of quaternary blends is usually 50–95 MPa, for total binder contents 450–910 kg/m^{3}and Portland cement replacement ratios between 30 % and 70 %. SCC quaternary blends containing fibres are not common in the literature [89–91], and the authors did not cite any publications where a fibre reinforced quaternary blend SCC achieved high strength. To achieve environmental sustainability through reducing the carbon footprint of concrete, this study aims to design high strength or ultra-high strength basalt fibre reinforced quaternary SCC mixes, containing Portland cement, SF, MK and LS, and to study their mechanical and durability related properties (i.e. sorptivity and absorption) as well as their microstructure and behaviour after exposure to elevated temperatures.

3. Experimental program

3.1. Raw materials

Four types of active and inert fillers from local sources were used in this study, namely, Portland cement, SF, MK and LS. Portland cement was CEM I (52.5) satisfying ASTM C150 [92] whereas SF with silica content equals to 96 % was in accordance with ASTM C1240 [93]. All powder characteristics are listed in Table 2. Both SF and MK were used as a pozzolanic (active) cement replacement material (Type II) while LS powder is considered as inert cement replacement material (Type I) according to the European Guidelines for SCC [7]. Quartz powder (QP) was used as a filler to partially replace fine aggregate to optimise the packing density of the mixes. QP was produced locally by grinding pure sand with high SiO$_2$ content. Particle size distribution of the used powders is illustrated in Fig. 1. Fraction Retained on 45 μm sieve was less than 1 % and the moisture content was less than 0.5 %. A high range water reducer admixture in accordance with ASTM C 494 [94] type G was used to achieve SCC requirements. Two sizes of basalt aggregate were used in this study, namely, Size 1 passing from sieve 10 mm and retained on 4.75 mm, and Size 2 passing from 4.75 mm and retained on 2.36 mm. The basalt aggregate mixture contained 70 % of Size 1 % and 30 % of Size 2. The used aggregates were saturated surface-dry (SSD). Water absorption, specific gravity, and maximum grain size were 1.71 %, 2.7, and 10 mm, respectively. Natural sand used had water absorption, specific gravity, and maximum grain size of 0.65 %, 2.81, and 2.36 mm, respectively. The sieve analysis grading curves of the used fine and coarse aggregates are presented in Fig. 1. Chopped basalt fibres (BF), were manufactured in China. Tap water was used in the mixing and curing processes.

Table 2
Chemical composition and physical properties for the used fillers.

| Compound (%)	OPC	SF	MK	LS	QP
SiO$_2$	21.20	96.0	55	3.61	99.20
AL$_2$O$_3$	5.50	0.10	42.7	0.33	0.35
Fe$_2$O$_3$	3.20	1.0	1.40	0.18	0.04
CaO	63.4	0.20	0.30	53.26	0.15
MgO	0.70	0.15	0.30	0.85	0.02
SO$_3$	2.40	0.10	0.01	0.050	–
Na$_2$O	0.10	0.10	0.30	0.02	0.01
K$_2$O	0.50	0.20	0.0	0.36	0.01
loss on ignition	3.00	2.15	0.90	41.34	0.2
Colour	Grey	Light grey	Light beige	white	white
Grain Size	90 μm	1 μm	0.50 μm	20 μm	45 μm
Specific Gravity	3.15	2.15	2.5	2.65	2.70
Bulk Density (t/m^3)	1.45	0.355	1.2	1.0	1.28
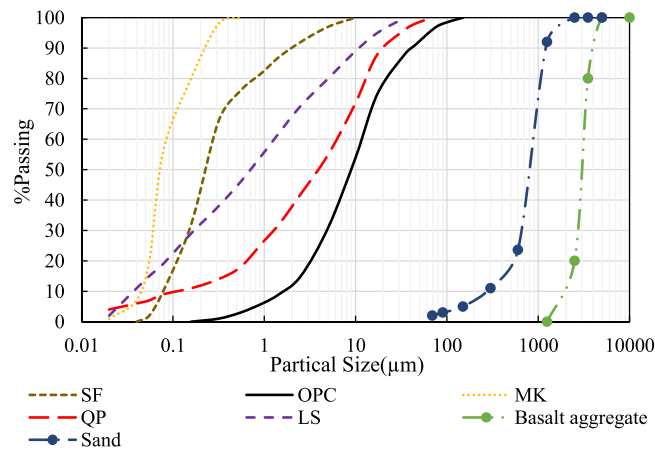
Fig. 1. Particle size distribution of used materials.

3.2. Concrete mix design

The authors conducted several trials to produce mixes in accordance with European SCC Guidelines 2005 [7], with the aim of achieving ultra-high compressive strength and acceptable fresh properties. Table 3 shows the proportions of nine mixes designed to be UHSFRSCC to achieve concrete strengths between 110 and 135 MPa. All these concrete mixes had the same total active and inert powder content of 1100 kg/m³, Basalt coarse aggregate content of 540 kg/m³ and Basalt fibre of 8.1 kg/m³ (0.3 % by volume). The nine mixes are divided into 3 groups. Each group included 3 mixes. In the first group, G1, the sand was replaced by 34 % QP and the cement was replaced by 20 % active powder (SF and/or MK). The first mix (M1) incorporated 20 % SF as cement replacement, while in mixes M2 and M3, SF was 15 % and 10 %, whereas MK was 5 % and 10 %, respectively. In the second group, G2, 20 % of the cement was replaced by the same replacement ratios of SF and MK as in the mixes in G1, and an additional 20 % was replaced by LS. No QP was used in G2 to replace sand. In the third group, G3, the cement was replaced by SF, MK and LS as in the mixes of G2, but in addition sand was replaced by 34 %QP in the three mixes. The water/ binder was kept constant as 0.182 (water content 200 kg/m³), the ratio of fine/total aggregate was 0.52 (between 0.48 and 0.55 in accordance with the European Guidelines for SCC [7]). The dosage of superplasticizer (SP), ranged between 3.5 % and 4.1 % by weight of total powder, in order to satisfy the workability requirements of the European Guidelines for SCC [7]. The mix codes, shown in Table 3 are based on SF and MK contents. For example, S15M5 represent concrete mix containing 15 % SF (S15) and 5 % MK (M5) as active fillers. The mix numbers are used to distinguish the mixes in the different groups.

3.3. Mixing, casting and curing processes

The mixing process was performed using a mechanical drum concrete mixer of 10 liters capacity. The mixture components were carefully weighted. Basalt aggregates, sand (natural or QP when used) and cement were first added to the mixer and thoroughly mixed. Cement replacement powders (SF, MK, LS) and basalt fibres were then added to the mix. The water and superplasticizer were finally added to the dry contents in the drum and mixed till the mixture achieved suitable consistency to be cast (mixing time differed according to components). From each of the concrete mixtures, 6 cubic specimens (100 mm) and 10 cylindrical specimens (diameter 100 mm, height 200 mm) were cast. Each mould was filled with concrete in three layers and each layer was lightly vibrated to remove

Table 3
Concrete mixes used in the current investigation (kg/m³).

M#	Group	Code	OPC	SF	MK	LS	CA	FA	QP	SP	BF	PV%
M1	G1	S20M0	880	220	0	0	540	390	200	40	8.1	0.56
M2	QP	S15M5	880	165	55	0	540	390	200	42	8.1	0.56
M3		S10M10	880	110	110	0	540	390	200	44	8.1	0.56
M4	G2	S20M0	660	220	0	220	540	590	0	39	8.1	0.57
M5	LS	S15M5	660	165	55	220	540	590	0	41	8.1	0.57
M6		S10M10	660	110	110	220	540	590	0	43	8.1	0.56
M7	G3	S20M0	660	220	0	220	540	390	200	41	8.1	0.57
M8	QP+LS	S15M5	660	165	55	220	540	390	200	43	8.1	0.56
M9		S10M10	660	110	110	220	540	390	200	45	8.1	0.56

M# = Mix number, OPC = Ordinary Portland Cement, LS = Limestone, SF = Silica Fume, MK = Metakaolin, CA = Basalt Coarse Aggregate, FA = Sand Fine Aggregate, QP = Quartz Powder, W = Water, SP = Superplasticizer, BF = Basalt fibre, PV = Paste volume, G1 = group containing QP as sand replacement, G2 = group containing LS as inert filler and G3 = group containing both QP and LS.

air voids. Finishing the concrete surface of the moulds was carried out and then the specimens were covered with plastic sheets to prevent water evaporation. After 48 h the specimens were demolded and cured in controlled hot water (75 °C ± 2 °C) for 3 days to accelerate the rate of strength gain [95]. Then the specimens were left in the curing tank at 25 °C ± 2 °C for 25 days until the age of testing at 28 days.

3.4. Furnace heating regime for the samples that were tested after exposure to elevated temperatures

At the age of 28 days, the specimens, to be heated, were taken from the tank and dried in an oven for two days at a temperature of 105 °C, to reduce their moisture, before subjecting them to higher elevated temperature in an electric muffle furnace (maximum temperature 1200 °C) in order to minimise the possibility of explosive failure [96]. For the elevated temperatures cycle, the heating rate was 5 °C/minute. To ensure homogeneous heating for each specimen, a distance of 20 mm was kept between specimens as shown in Fig. 2(a). Elevated temperatures of 200 °C, 300 °C were considered as over-heating conditions for concrete. These temperatures were selected since the temperature of fire flames in open air was reported to be in the range of 320–400 °C [97–99]. Once the required temperature was reached, the samples were kept at this temperature for 1 h to ensure a uniform heating for each sample [99]. At the end of each exposure period, the power was turned off and the specimens were allowed to slowly cool inside the furnace, while keeping the furnace door closed to prevent possible development of a thermal gradient in the specimens. The exposure temperature–time relationship is shown in Fig. 2(b).

3.5. Testing procedures

3.5.1. Fresh characteristics
SCC fresh properties were evaluated namely: flowability, viscosity and passing ability using slump flow, V-funnel, and L-Box tests, respectively. In slump flow, the diameter of the fresh SCC is measured in two directions and the average diameter is recorded as slump flow diameter (Sf). V-funnel test can measure the indirect viscosity of SCC mixtures based on the elapsed time between the beginning and end of flowing of SCC from the funnel (Tv). In the L-Box test, the fresh SCC in the vertical box is allowed to flow through the bars to the horizontal box. When the flow stops, the ratio (h_2/h_1) is measured, where h_2 is the length of the SCC in the horizontal box, and h_1 is the height of the remaining concrete in the vertical box. This is called (PA ratio) denoting the passing ability of SCC.

3.5.2. Mechanical properties
Compressive strength test was performed on 100 mm cubes according to BS EN 12390 3:2019 [100] using ELE digital testing machine of 2000 ton maximum capacity. Splitting tensile strength was recorded for cylindrical specimens of 100 mm diameter and 200 mm height according to ASTM C496/C496M [101].

3.5.3. Ultrasonic pulse velocity test
Ultrasonic pulse velocity test was conducted on 100 mm cubes in accordance with ASTM C597 [102]. This test was used to assess the concrete quality by monitoring the time required for the wave to pass through a concrete cube between a transmitter and receiver. The cube side length is accurately measured using a Vernier Caliper, the velocity is calculated and recorded in µs.

3.5.4. Permeation properties
Water absorption by capillary action (sorptivity) and water absorption by total immersion was performed on 50 mm slices taken from the prepared cylindrical specimens according to ASTM C1585 [103] and ASTM C642 [104], respectively. To achieve a nearly constant mass, the specimens were dried in an oven for three days at a temperature of 50 °C. The slices were then sealed in bags for minimum 15 days. The tests were performed before and after exposure to elevated temperatures of 200 or 300 °C. After exposure to an elevated temperature, the specimens were cooled to room temperature and weighed. Mass change after semi-immersion for one hour was measured and the sorptivity was calculated and recorded in $g/mm^2/s^{1/2}$. Percentage water absorption was calculated after full immersion for 4 days.
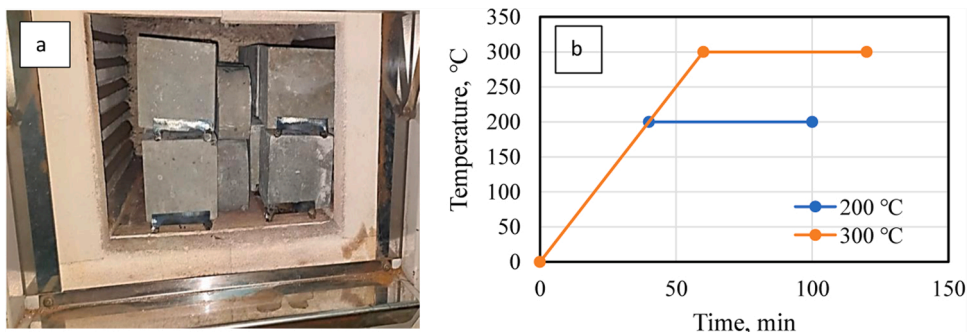

Fig. 2. Heating the test samples: (a) position of samples inside the furnace (b) heating curve.

3.5.5. Micro-structural properties

The morphology of selected specimens was investigated by scanning electron microscopy (SEM, Zeiss Sigma 500 VP Analytical FE-SEM, Inspect Carl Zeiss Company, Germany) with a maximum magnification of ($10 \times - 1,000,000 \times$) with resolution 0.8 nm. This SEM microscope is equipped with a unit for energy dispersive X-ray analysis Spectroscopy (EDX) for determination semi-quantitative elemental analysis of the hydrated phases.

3.6. Results and discussions

3.6.1. Fresh properties of UHSFRSCC

Table 4 shows the fresh properties for test mixes. It can be seen from Table 3 that the amount of superplasticizer added for each concrete mix slightly increased with increasing the amount of active and inert powders (SK, MK, and LS) to satisfy SCC workability requirement according to The European Guidelines for SCC [7].

For the same powder type and content, G2 and G3 mixes showed that utilisation of QP as a sand replacement reduced the fluidity of the mixes. However, rheological classes {flowability (SF3), viscosity (VF1) and passing ability (PA2)} were not affected due to their practically wide limits. Moreover, for the mixes in each group MK inclusion as a partial replacement of SF resulted in lower slump-flow values, higher V-funnel flow times and lower L-Box ratios compared to the SF concrete and the amount of reduction in the flowability, viscosity and passing ability increased with increasing MK content.

A pilot study was conducted to increase MK replacement level over that utilised in S10M10 mixes, up to 10 % by total powder weight as shown in Fig. 3. In spite of increasing the amount of superplasticizer, the mix failed to satisfy SCC requirement. Therefore, the content in S10M10 was considered to be the maximum for the mixes in the current study. Reduction in the flowability due to 10 % MK inclusion was 22 %, 8.75 % and 15.2 % for mixes M3, M6 and M9 compared with the mixes containing only SF in the same group (M1, M4 and M7), respectively. The significant reduction in rheological properties due to MK inclusion was reflected on SCC classes. On the contrary, inclusion of limestone powder (LS) as a partial replacement of cement (comparing G1 and G3 mixes), the flowability was slightly improved. As shown in Table 4, flowability of Mix M7 in Group G3 which contained 20 % SF as active powder, and 20 % LS as inert powder was 790 mm while the flowability of Mix M1 in Group G1 which contained only 20 % SF was only 770 mm. However, the flowability class was not changed. Therefore, LS incorporation has no significant negative effect on fresh properties of UHSFRSCC. This agrees with the results obtained by Zhu and Gibbs [105]. On the other hand, comparing the rheological characteristics of the mixtures containing MK in G1 and G3 reveals that not only the MK inclusion significantly decreased the flowability, but MK also affected the class of SCC.

It can be seen from Table 4 that flowability classes of M2 and M3 were SF2 and SF1, while they were upgraded to SF3 and SF2 for M8 and M9, respectively. This effect may be attributed to the higher specific surface area of MK compared to SF, as well as the irregular or plate like shape of MK particles [49 and 50]. The high improvement in fresh characteristics occurred in Mix M4 due to the presence of LS and absence of MK and QP, although this mixture had the least SP content as shown in Table 3. A similar observation was noted by [58]. The worst fresh characteristics were recorded for mixture M9, which contained 10 % MK as active powder and 34 % QP as sand replacement. It can be argued that this effect can be attributed to higher water demand due to the decreased particles size and the increased specific surface area of both MK (< SF) and QP (< sand). A similar effect was reported by other researchers [49,59,73,74].

3.6.2. Hardened properties of UHSFRSCC

hardened properties in terms of UPV, compressive and splitting tensile strength were determined for all concrete specimens at ambient temperature ($25 \pm 2\,^\circ$C) and after exposure to elevated temperature of 200 or 300 $^\circ$C. The results will be discussed in the following sections.

Table 4
Fresh properties for UHSFRSCC mixes.

M#	Group	Mix code	Flowability Slump flow (Sf), mm		Viscosity V-funnel (Tv), s		Passing ability L-Box (h2/h1) (PA ratio)	
			Value	Classification	Value	Classification	Value	Classification
M1	G1	S20M0	770	SF3	8	VF2	0.9	PA2
M2	QP	S15M5	730	SF2	11	VF2	0.85	PA2
M3		S10M10	600	SF1	12	VF2	0.8	PA2
M4	G2	S20M0	800	SF3	6	VF1	1	PA2
M5	LS	S15M5	780	SF3	8	VF2	0.97	PA2
M6		S10M10	730	SF2	9	VF2	0.9	PA2
M7	G3	S20M0	790	SF3	7	VF1	0.95	PA2
M8	QP + LS	S15M5	760	SF3	10	VF2	0.9	PA2
M9		S10M10	670	SF2	11	VF2	0.85	PA2
The European Guidelines for SCC [7]			550–800		8–25		≥ 0.8	
Classes			SF1	550–650	VF1	< 8	PA1	with 2 rebars
			SF2	660–750	VF2	8–25	PA2	with 3 rebars
			SF3	760–800				

(a) Slump flow and L box for mix containing 10% MK (M3) (accepted as SCC)

(b) Slump flow and L box for mix containing 15% MK (failed as SCC)
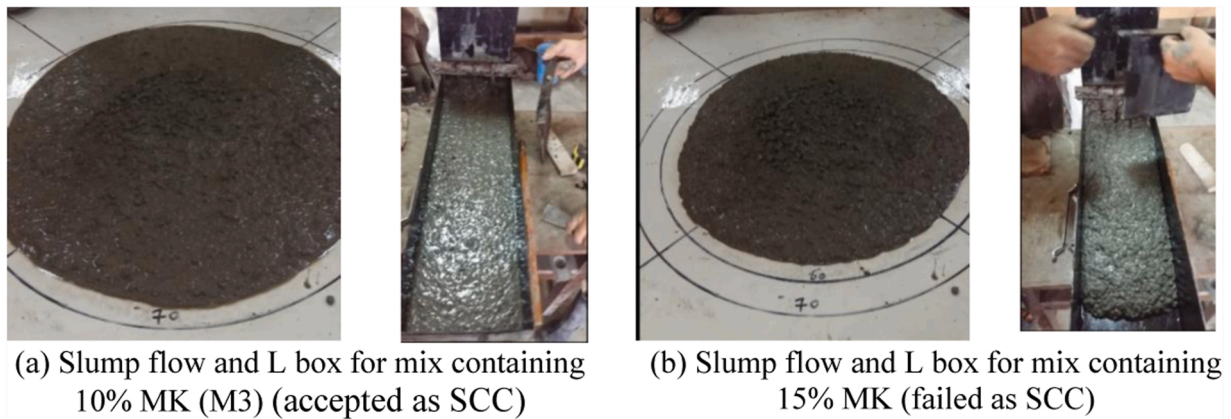
Fig. 3. Fresh properties for UHSFRSCC mixes containing 10 %MK and 15 %MK.

3.6.2.1. Nondestructive testing (Ultrasonic pulse velocity, UPV). UPV test results are reported in Table5 for all mixes at different exposure temperature conditions. When considering the quality of mixes in terms of UPV values, excellent quality of concrete has UPV greater than 4500 m/s; for good concrete the UPV is 3500–4500 m/s; for fair or medium concrete the UPV is 3000–3500 m/s, and for poor concrete UPV is less than 3000 m/s. It can be seen that all mixes, except those for G1 exposed to 300 °C can be classified as excellent quality concrete. It can be observed from Table 5 that UPV results decreased in all studied concrete with increasing temperature as a result of micro-cracks formation after elevated temperature exposure. On the other hand, UPV increased with inclusion of active and inert powder (MK and LS) which may be attributed to both physical micro filler and chemical pozzolanic effect of these powders as will be discussed later sections. Enhancement of UPV for SCC with additives was reported by Kannan and Ganesan [71].

3.6.2.2. Compressive strength. The compressive and splitting tensile strengths for all UHSFRSCC mixes at ambient temperature 25 °C and specified elevated temperatures 200 and 300 °C are reported in Table 5. The results indicate that the mechanical properties generally decreased with increasing elevated temperatures. However, the degree of strength degradation depends on the type and amount of the used active and/or inert powder as well as exposure temperature.

Table 5 includes the results of the compressive strength (CS) for all mixes at different exposure conditions. Fig. 4(a) shows CS of the test mixes at ambient temperature. It can be seen that, for each group, the inclusion of 5 % MK or 10 % MK resulted in slightly higher or lower compressive strength compared to that containing SF only in the same group, respectively. The percentage of strength improvement and reduction are less than 4.1 %. This observation is in agreement with the results found in previous studies [51,106, 107]. Moreover, the mixtures having QP and /or LS powder possess higher compressive strength, irrespective of the presence of active powder (MK or SF). The mixtures in G3 have higher compressive strengths than corresponding mixes in G1 and G2. Comparing mixtures in G1 and G3 indicates that LS inclusion increased the compressive strength of UHSFRSCC, and the average percentage of improvement was 6.3 %. On the other hand, comparing mixes in G2 and G3 shows that replacing 34 % sand with QP somewhat increased the average compressive strength by 2.5 %. The improved mechanical and durability properties of concrete containing fine powder (QP and LS) may be attributed to its pore-filling effect which led to a densified and more compacted microstructure [50,105, 108]. In addition, Tikkanen et al. [60] suggested that the inert fillers enhance the hydration by acting as nucleation sites for C-S-H and thus become a part of the binder matrix.

It can be seen from Table 5 that the compressive strength results for G1, G2 and G3 concrete groups ranged between 115.8–124.4 MPa, 121.3–128.3 MPa, and 124.2–132.3 MPa, respectively. The concrete containing (5 % MK + 15 % SF + 20 % LS) as a cement replacement and 34 % QP as a sand replacement, Mix M8, had the highest compressive strength of 132.3 MPa. On the other hand, Mix M3 in G1 had the lowest compressive strength of 115.8 MPa. The enhanced compressive strength of MK blended UHSFRSCC

Table 5
Mechanical properties and UPV of UHSFRSCC at ambient temperature and after exposure to elevated temperatures.

| M#	Group	Mix code	Temp, 25 °C			Temp, 200 °C			Temp, 300 °C		
			CS, MPa	STS, MPa	UPV, km/s	CS, MPa	STS, MPa	UPV, km/s	CS, MPa	STS, MPa	UPV, km/s
M1	G1	S20M0	120.71	13.60	5.21	111.05	12.51	4.79	101.39	11.42	4.38
M2	QP	S15M5	124.37	14.60	5.26	112.42	13.70	4.82	104.47	12.60	4.42
M3		S10M10	115.83	13.10	5.19	113.56	12.45	4.93	105.97	11.86	4.45
M4	G2	S20M0	124.52	14.30	5.26	117.05	13.44	4.94	109.57	12.35	4.63
M5	LS	S15M5	128.34	15.30	5.30	118.64	14.30	5.01	112.94	13.60	4.66
M6		S10M10	121.29	14.10	5.23	119.19	13.80	5.10	113.10	12.95	4.70
M7	G3	S20M0	127.06	14.60	5.29	121.98	14.30	5.08	115.62	13.10	4.81
M8	QP + LS	S15M5	132.31	15.90	5.36	122.02	15.10	5.10	120.40	14.60	4.87
M9		S10M10	124.22	14.60	5.27	123.29	14.40	5.21	120.90	13.90	4.93
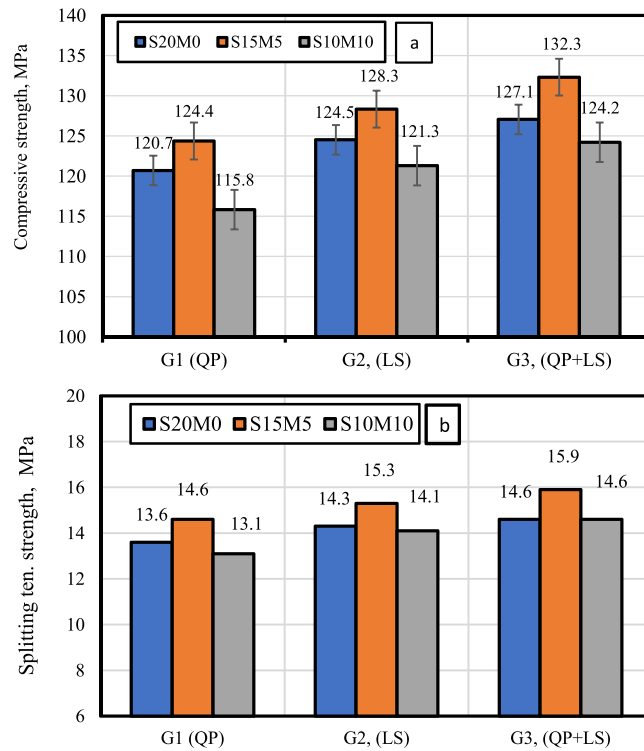
Fig. 4. The mechanical properties of control specimens, (a) compressive (b) splitting tensile strength.

is mainly due to quick pozzolanic reaction of MK, the acceleration of OPC hydration as well as its micro-filler effect due to its high surface area [52,109]. However, a further increase in replacement level of cement with MK resulted in an increase of the unreacted alumina silicate in the mixture due to insufficient presence of Portlandite [52]. These results are in agreement with the findings of
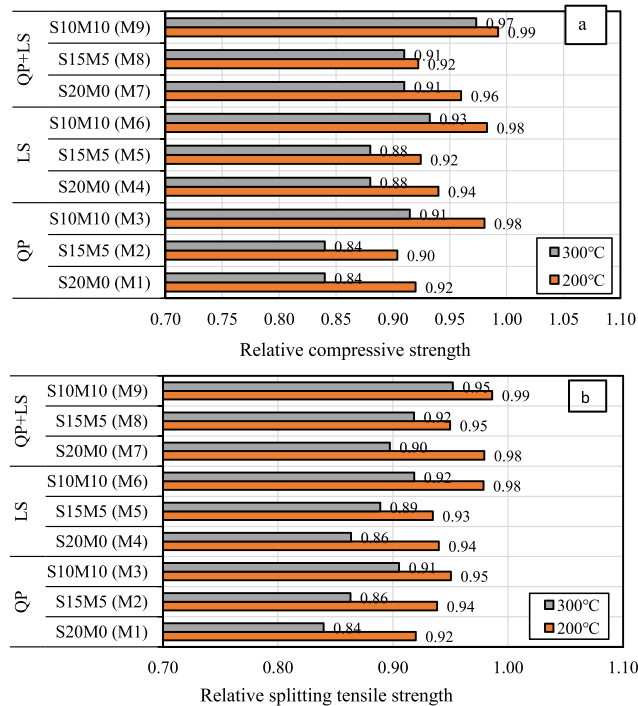

Fig. 5. Relative strength after temperature exposure (a) (RCS), $(f'_c)_T/(f'_c)_{25}$, (b) (RSTS), $(f'_t)_T/(f'_t)_{25}$.

other researchers who also noted that there is an optimum level of cement replacement with MK [65,74]. Salari et al. [18] reported that 42 %, 24 %, 23 % and 11 % of the publications designed SCC with compressive strengths in the range of 50–70 MPa, 75–100 MPa, 100–125 MPa and > 150 MPa (Ultra High Performance), respectively. He did not cite any studies where the SCC compressive strength achieved 125–150 MPa. Therefore, mixes with similar strengths to those exhibited by S15M5 in G2 and G3 are novel.

Fig. 5(a) presents the relative compressive strength (RCS), which is the ratio of compressive strength after a particular exposure temperature, $(f'_c)_T$, to that of specimens tested at ambient temperature, $(f'_c)_{25}$. It should be noted RCS for all mixtures was (0.9–0.99) at 200 °C and (0.84–0.97) at 300 °C. These results are in agreement with Uysa [67], who reported a small decrease in the compressive strength of SCC samples containing up to 30 %LS heated to 200 °C. However, some reports in the literature indicated an increase in the compressive strength upon exposure to temperatures in the range of 200–300 °C [65,66]. They attributed this to the progressive pozzolanic reaction of residual unreacted MK and/or SF particles as a result of temperature rise. This phenomenon is called internal autoclaving by steam in the concrete pores. This was not exhibited in the current study, as the samples were dried for two days at a temperature of 105 °C prior to exposure to elevated temperatures. Therefore, not enough steam was generated to help with the continued hydration.

It is clearly observed from Fig. 5(a) that the RCS increased with incorporating QP and/or LS as well as with increasing MK content. LS addition improved RCS by 1.2–4.2 % and 6.0–7.7 % after exposure to 200 and 300 °C, whilst QP addition slightly improved RCS by 1.0–2.1 % and 3.3–4.2 % after exposure to 200 and 300 °C, respectively. Moreover, incorporating 5 %MK decreased RCS by 1.7–3.9 % after exposure to 200 °C while it had no effect after exposure to 300 °C. Alternatively, incorporating 10 %MK improved RCS by 3.4–6.6 % and 6–9 % after exposure to 200 and 300 °C, respectively. It is clear that mix M9 possessed the best resistance to compressive strength degradation under elevated temperatures. RCS was increased by 7.9 % and 15.9 % with the presence of 20 %LS and10 %MK, in M9 compared with M1 after exposure to 200 and 300 °C, respectively. Incorporating combined 20 %LS and 10 %MK minimised the losses of compressive strength by 1–3 % after exposure to 200 and 300 °C, respectively. This is in agreement with the findings of other publications, in which QP addition was found to enhance the residual mechanical properties after exposure to elevated temperature [68], and similar effects were noted for the inclusion of LS [67] and MK [65,66].

3.6.2.3. Splitting tensile strength. Development of an adequate tensile strength is crucial for elevated temperature behaviour as it prevents explosive failure and cracking of concrete, by resisting thermal stresses, produced due to internal vapour pressures at high temperature (300–500 °C) [25]. Table 5 and Fig. 4(b) show the results of splitting tensile strength of specimens. Splitting tensile strength (STS) follows a similar trend as the compressive strength. STS decreased with increasing elevated temperature for all studied concretes up to 300 °C. The results reported in Table 5 show that inclusion of 5 %MK resulted in enhancement of STS, while the addition of 10 % MK had an adverse or no significant effect, compared to the 20 % SF specimens without MK. Adding LS enhanced the STS compared with samples containing QP. However, combination of both powders (LS and QP) produced the best performance. In addition, the percentage of improvement increased with increasing exposure temperature. For example, S15M5 mix exhibited an improvement of STS by 7.4, 6.99, 8.9 % compared with mixes containing 20 %SF without MK in G1, G2 and G3, for samples at 25 °C, respectively. The improvement was 9.5, 6.4, 5.6 % at 200 °C and was 10.3, 10.1, 11.5 % at 300 °C, respectively. Moreover, utilising both QP and LS, resulted in improvement of STS by 7.4 %, 14.3 % and 14.7 % for specimens at 25, 200 and 300 compared to mixes with QP only, respectively.

Relative splitting tensile strength (RSTS) for all designed concretes after temperature exposure is presented in Fig. 5(b). There is some increase in RSTS with mixes containing MK and LS, compared to mixes with SF and QP. Moreover, increasing the elevated temperature resulted in a reduction of RSTS. It was found that maximum RSTS were observed for samples containing combined 10 %

Table 6
Sorptivity and absorption of UHSFRSCC at ambient temperature and after exposure to elevated temperatures.

M#	Group	Mix code	Temp, 25 °C		Temp, 200 °C		Temp, 300 °C	
			Sorptivity g/mm^2/s$^{0.5}$	Absorption %	Sorptivity g/mm^2/s$^{0.5}$	Absorption %	Sorptivity g/mm^2/s$^{0.5}$	Absorption %
M1	G1 QP	S20M0	0.0135	0.31	0.0165	0.36	0.0175	0.43
M2		S15M5	0.0125	0.30	0.0150	0.34	0.0170	0.39
M3		S10M10	0.0150	0.35	0.0160	0.35	0.0170	0.41
M4	G2 LS	S20M0	0.0120	0.28	0.0135	0.33	0.0150	0.39
M5		S15M5	0.0095	0.25	0.0120	0.31	0.0135	0.34
M6		S10M10	0.0120	0.31	0.0125	0.32	0.0140	0.36
M7	G3 QP + LS	S20M0	0.0100	0.26	0.0110	0.28	0.0130	0.34
M8		S15M5	0.0080	0.22	0.0100	0.25	0.0107	0.29
M9		S10M10	0.0110	0.26	0.0115	0.29	0.0120	0.34

MK + 20 %LS (M9), where RSTS was improved by 7.2 % and 13.4 % compared to the reference mixture (M1) containing SF and QP, after exposure to 200 and 300 °C, respectively. RSTS decreased at temperature beyond 200 °C. However, the amount of reduction decreases with incorporating both MK and LS powder. This may be attributed to the improved microstructure of interfacial transition zone (ITZ) around both aggregate particles as well as basalt fibre due to the higher pozzolanic activity of MK and the filling effect of LS [66]. Moreover, MK was found to be essential for initial strength gain until 28 days [87]. STS loss were only 8 % and 5 % for samples containing 5 %MK and 10 %MK at 300 °C elevated temperature for mix M8 and M9, respectively.

3.6.3. Durability related properties (sorptivity and absorption)

Exposure of concrete to elevated temperatures leads to the development of micro-cracks and pores, which have a major impact on permeation characteristics such as water absorption and sorptivity [110–113]. In general, the permeation characteristics are considered as durability indicators [114]. To study the designed UHSFRSCC at different exposure temperatures, water sorptivity and absorption were assessed, and the results are reported in Table 6.

3.6.3.1. Sorptivity. It can be seen from the results reported in Table 6 that sorptivity decreased with incorporating both QP and LS powder which may be attributed to the physical micro filler effect of these fine powders. In addition, sorptivity decreased with adding 10 %MK and decreased significantly with adding 5 %MK. This may be attributed to the higher pozzolanic activity of MK resulting formation of more gels that fill micropores in the matrix. For mixes containing combined QP and LS such as M7, sorptivity decreased by 26 % and 17 % compared to that of mixes containing separate powder either QP (M1) or those containing LS (M4), respectively. Furthermore, adding 5 %MK in mix M8 resulted in reducing the sorptivity by 20 % compared to that of the mix M7. Similarly, Gesoglu et al. [108] reported that the sorptivity coefficients for ternary mixtures were less than those of binary mixtures. However, their values for sorptivity were between 0.05 and 0.065 for ternary mixes with fly ash and marble powder or Limestone powder. These values were much higher than those recorded in the current investigation. This can be attributed to the fact that the current study employed a total filler content of 1100 kg/m^3, whereas Gesoglu et al. [108] used only 520 kg/m^3 in their mixes. Therefore, the incorporation of higher filler contents in the current investigation dramatically enhanced the sorptivity.

In general, sorptivity is expected to increase with exposure to elevated temperature, as a result of the formation of surface micro-cracks, allowing water to penetrate the concrete. Moreover, Ling et al. [115] argued that moisture loss during the drying and subjecting the concrete to elevated temperatures will lead to higher sorptivity for heated samples compared to unheated ones. However, MK was found to help during exposure to elevated temperature. For example, mixes in G1, with 5 % MK exhibited an increase in sorptivity of only 20 %, compared to the mix without MK which suffered 22.2 % increase in sorptivity when heated to 200 °C. Arslan et al. [116],
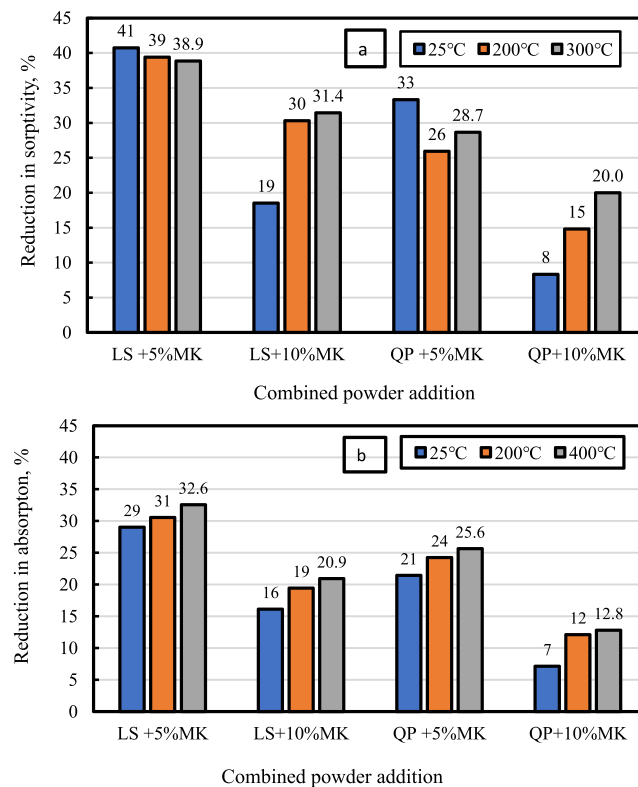

Fig. 6. Effect of combined powder addition on reduction of (a) Sorptivity, (b) Absorption compared to a mix with 20 % SF and no MK at different temperatures.

Karatas et al. [117] also found that the sorptivity behaviour was improved for SCC with MK after exposure to elevated temperature.

The sorptivity values of M8 were lower than those of M1 by 41 %, 39 % and 38.9 % for ambient, 200 °C and 300 °C, respectively. These results show the positive effect of combined inert and active fillers on sorptivity in all temperature conditions. Fig. 6(a), represents effect of MK addition along with other fillers (MK+LS or MK+QP) on the reduction of sorptivity at different temperatures
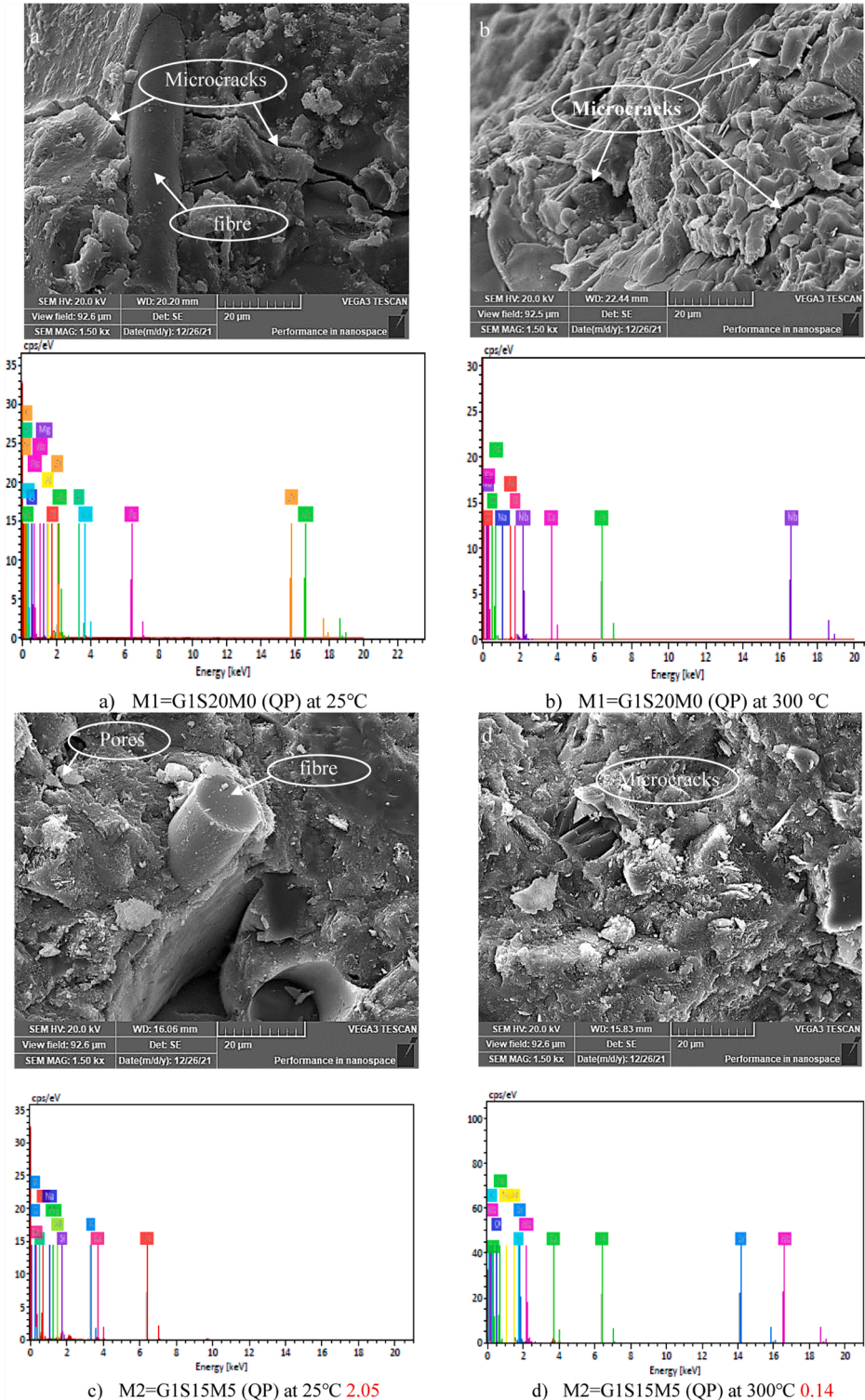

a) M1=G1S20M0 (QP) at 25℃

b) M1=G1S20M0 (QP) at 300 ℃

c) M2=G1S15M5 (QP) at 25℃ 2.05

d) M2=G1S15M5 (QP) at 300℃ 0.14

Fig. 7. SEM for samples M1 and M2 at both 25 °C and 300 °C.

compared with the counterpart mix containing 20 % SF only without MK. It can be seen from the figure that, generally, all combined powder inclusions decreased sorptivity of samples subject to different elevated temperatures up to 300 °C. However, combined 20 % LS + 5 %MK possessed the maximum reduction in sorptivity at different exposure temperatures.
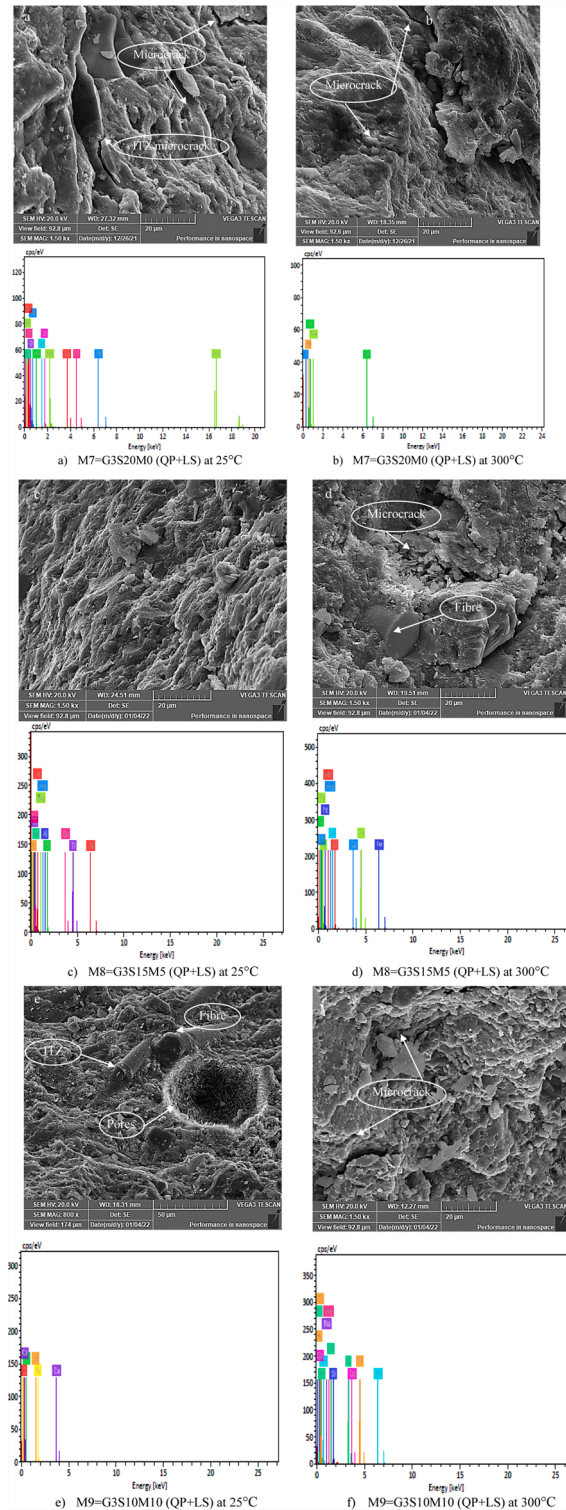

Fig. 8. SEM for samples M7, M8 and M9 at both 25 °C and 300 °C.

3.6.3.2. Absorption. Results of water absorption of all test specimens are presented in Table 6 and Fig. 6(b). It can be observed from the table that the water absorption increased with increasing the elevated temperature, and this is in agreement with the previous studies [52]. On the other hand, water absorption decreased with incorporating QP and LS powder in the mixes. In addition, water absorption decreased significantly with 5 %MK inclusion, however, with 10 %MK the absorption was higher than that for the samples with 5 % MK. For example, water absorption for M7 was reduced by 16.1 % and 7.1 % compared to that of M1 and M4, respectively. Furthermore, presence of 5 %MK in M8, resulted in a reduction of water absorption by 15.4 % compared to M7, which does not contain MK. Like sorptivity results, overheating of specimens to 200 °C and 300 °C resulted in an increase of water absorption of the specimens. However, the inert powders were helpful in reducing the effect of heat as can be seen from Table 6. Similar trends were reported by da Silva and de Brito [70] when studying the absorption of SCC binary and ternary mixes with LS and fly ash. However, all their absorption values were above 10.5 %, whereas in the current investigation the maximum recorded absorption was 0.43 %. Again, this can also be attributed to the increased packing density of the mixes employed herein due to the higher binder content and careful selection of mix ingredients.

Fig. 6(b) represents the effect of the addition of MK along with other fillers on reduction of water absorption at different exposure temperatures compared with the containing 20 % SF without MK. It can be seen from the figure that, generally, combined powder decreased water absorption of concrete subjected to different elevated temperature up to 300 °C. However, combined 20 %LS + 5 % MK possessed the maximum reduction in absorption at different exposure temperatures.

3.6.4. Microstructure of studied specimens

The SEM images of selected samples (M1, M2 in G1 and M7, M8, M9 in G3) at ambient and 300 °C elevated temperatures are shown in Figs. 7 and 8. It can be seen from Fig. 7-a that the concrete containing only SF (M1) at 25 °C exhibited some cracks. Basalt fibres are seen to bridge the gaps and micro-cracks within concrete, resulting in the high strength [25]. The observed cracks may be attributed to the thermal expansion and drying shrinkage as a results of higher cement content (880 kg/m^3). The number and width of these micro-cracks increased with increasing thermal expansion due to exposure to elevated temperature (300 °C) as shown in Fig. 7-b. This was reflected on degradation in strength and permeation characteristics [25]. Fig. 7-c, and d show SEM images for specimen containing 5 % MK combined with 15 %SF (M2) at 25 °C and 300 °C, respectively. It can be observed that, at ambient temperature, the bulk matrix was more densified, and cracking was less than that in the 20 % SF mix without MK (M1) in Fig. 7-a. This could be attributed to the high reactivity of MK at the early ages compared to SF which leads to formation of high amount of C-S-H and C-A-H gels. As a result, strength and permeation properties were enhanced. When a specimen from the same mix was exposed to 300 °C (Fig. 7-d); the sample still exhibited a dense internal structure while a few micro-cracks and pores were detected. These observations were confirmed through EDX analysis where, Si/Ca ratio of concrete (M2) incorporating combined (5 %MK + 15 %SF) has shown higher value compared to SF concrete (M1) at 25 °C and 300 °C, and this also explains the observed increased compressive strength at different temperatures for this mix compared with M1.

SEM images of concrete specimens containing LS, QP as inert powders beside SF and/or MK are shown in Fig. 8(a–f) at both ambient and 300 °C elevated temperatures. Specimens incorporating LS powder (M7 and M8) showed a denser microstructure with limited number of microcracks compared with mixes without LS (M1 and M2). This could be attributed to the pore filler effect as well as the contribution of synergic effect of MK and LS in enriching the amount of hydration products by consuming C-H as well as the formation of carbo-aluminate after 28 days [118]. Besides, the drying shrinkage was probably reduced as a result of higher cement replacement level (40 %). This may explain the higher residual strength and permeation properties. Moreover, SEM images for SF concrete specimens, M7 (Fig. 8-a), showed a higher number of micro-cracks than that incorporating combined SF/MK, M8 (Fig. 8-c) at ambient temperature. EDX analysis reveals that Si/Ca ratio for concrete incorporating 15 %SF + 5 %MK (M8) is higher than that of 20 %SF concrete (M7) at ambient temperature. Therefore, the microstructure of M8 was denser than that of M7. The enhanced microstructure is consistent with strength and permeation results. On the other hand, the microstructure as shown in Figs. 8-b and 8-d exhibited signs of degradation at elevated temperature as a result of the deterioration of C–S–H and/or C-A-H gels, explaining the observed reduction in compressive strength. The specimens containing combined SF/MK showed less microcracking than those incorporating SF only. SEM images for concrete specimens incorporating combined 10 %SF and 10 %MK (M9) are shown in Fig. 8-e and -f at ambient temperature and at 300 °C. It can be seen from Fig. 7-e that specimens show a less dense microstructure with some pores at ambient temperature than the sample with SF only (M7). However, at 300 °C (Fig. 8-f) this specimen had a smaller number of microcracks and pores than the sample with SF only (M7) (Fig. 8-b). EDX analysis confirm that Si/Ca ratio for concrete incorporating 10 %SF + 10 %MK (M9) is less than that of 20 %SF concrete (M7) at ambient temperature while the case was reversed at 300 °C. This complies with strength and permeation characteristics and clarifies the role of MK in increasing the resistance of concrete to elevated temperature exposure.

4. Conclusions

Using active and inert fillers from local sources in Egypt, binary, ternary or quaternary UHSFRSCC mixes were designed. The maximum cement replacement ratio reached 40 %, and in some mixes QP was used to partially replace 34 % sand to improve the matrix packing density. Based on the results the following conclusions can be drawn:

1. SCC mixes, with compressive strengths exceeding 115 MPa, were produced. Amongst these mixes, two quaternary blends containing 15 % SF, 5 % MK, 20 % LS as partial Portland cement replacements, with or without partial replacement sand with QP,

achieved a compressive strength > 125 MPa, a level of strength not cited for quaternary SCC in published literature. All fillers, both active and inert, co-operated to realise this level of strength.

2. Regarding the mix containing only 20 % SF, replacing 5 %SF by 5 %MK and incorporating 20 %LS these combined blends improve compressive and splitting tensile strength by 10 % and 17 % respectively at ambient temperature while, these percentages reach to 19 % and 28 % respectively after exposure to 300 °C.

3. The inclusion of 20 % LS improved both the fresh and mechanical properties of UHSFRSCC at all temperature conditions.

4. Mixes containing 10 % MK, as Portland cement replacement, exhibited impaired fresh and compressive strength, compared to mixes with only 5 % MK. The tensile strength was not significantly affected. However, the higher MK mixes exhibited improved strength retention after exposure to elevated temperature.

5. Partially replacing sand with 34 % QP adversely affected the fresh properties, but the mechanical strength both at room temperature and after exposure to elevated temperature were marginally improved due to the inclusion of QP.

6. Mixes with 5 % MK exhibited improved tensile strength, compared to mixes with 20 % SF only, at all temperature conditions. Remarkably, the improvement was higher for the higher exposure temperature. Mixes with both LS and QP exhibited the highest splitting tensile strength at all temperature conditions.

7. Quality of UHSFRSCC containing 20 % active mineral admixture (SF and MK) and 20 % inert powder (LS) as cement replacement with and/or without QP as sand replacement, can be classified as excellent concrete even after exposure to 300 °C, since the UPV values exceeded 4500 m/s. While UHSFRSCC which contains only 20 % active mineral admixture and does not contain LS can be classified as excellent at ambient temperature even after exposure to 200 °C while, can be considered as good concrete after exposure to 300 °C as UPV values declined below 4500 m/s.

8. The ternary and quaternary blends designed in this study exhibited very low sorptivity and absorption values compared to the mixes cited in the literature due to the higher powder content and the efficient packing density. The sorptivity and absorption were 0.008 % and 0.22 %, respectively, for a mix containing 15 % SF, 5 % MK, 20 % LS and 34 % QP as sand replacement.

9. The SEM images explained the recorded results for hardened properties and permeation characteristics.

5. Scope for future work

It can be concluded that the incorporation of both active and inert mineral powders as partially cement replacement not only enhances the engineering properties of UHSFRSCC and reduces permeation properties but also improves the microstructure of the composite. Future works on UHSFRSCC incorporating other different types of active (fly ash, GGBS) and inert powder like (Basalt) powders are recommended for the enhancement of mechanical properties. Effect of higher elevated temperature over 300 °C on other residual properties (flexure, modulus of elasticity) of UHSFRSCC need to be investigated. Influence of improvement of UHSFRSCC ductility by the addition of microfibers need investigation. For the application, structural behaviour of reinforced UHSFRSCC containing blended active and inert powders and microfiber under axial, flexural loads should be assessed in future research.

CRediT authorship contribution statement

Mohamed S. Saif: Mix design; experimental design; supervision of the trial mixes; supervision of experimental work; Data curation, Writing – original draft. **Ali S. Shanour:** Student academic adviser. **Gamal E. Abdelaziz**: Visualization; revision of the mix design; facilitating lab work. **Hanaa Elsayad:** Writing – review & editing. **Ibrahim G. Shaaban:** Analysis and discussion of results; final revision of the manuscript. **Bassam A. Tayeh:** Writing – review & editing; corresponding author. **Mahmoud S. Hammad:** Carrying out trial mixes; carrying out the experimental work; designing graphs and tables.

Declaration of Competing Interest

The authors declare that they have no known competing financial interests or personal relationships that could have appeared to influence the work reported in this paper.

Data Availability

Data will be made available on request.

Acknowledgements

References

[1] S. Dey, V.V. Praveen Kumar, K.R. Goud, S.K.J. Basha, State of art review on self-compacting concrete using mineral admixtures, J. Build. Pathol. Rehabil. (2021) 6–18, https://doi.org/10.1007/s41024-021-00110-9.

[2] H. Okamura, M. Ouchi, Self-compacting concrete, J. Adv. Technol. 1 (2003) 5–15, https://doi.org/10.3151/jact.1.5.

[3] A. Skarendahl, P. Billberg, Casting of self compacting concrete, RILEM Tech. Comm. 188-CSC (2006).

[4] S.-H. Kang, S.-G. Hong, J. Moon, The use of rice husk ash as reactive filler in ultra-high-performance concrete, Cem. Concr. Res. 115 (2019) 389–400, https://doi.org/10.1016/j.cemconres.2018.09.004.

[5] D.-Y. Yoo, I. You, Liquid crystal display glass powder as a filler for enhancing steel fibre pullout resistance in ultra-high-performance concrete, J. Build. Eng. 33 (2021), 101846, https://doi.org/10.1016/j.jobe.2020.101846.

[6] M. Courtial, M.-N. de Noirfontaine M, F. Dunstetter, M. Signes-Frehel, M. Mounanga, K. K. Cherkaoui, A. Khelidj, Effect of polycarboxylate and crushed quartz in UHPC: microstructural investigation, Constr. Build. Mater. 44 (2013) 699–705, https://doi.org/10.1016/j.conbuildmat.2013.03.077.

[7] EFNARC, Specification and Guidelines for Self-Compacting Concrete, 2002.

[8] N.M. Azmee, N. Shafiq, Ultra-high-performance concrete: from fundamental to applications, Case Stud. Constr. Mater. 9 (2018), https://doi.org/10.1016/j.cscm.2018.e00197.

[9] Y. Chen, R. Yu, X. Wang, J. Chen, Z. Shui, Evaluation and optimization of Ultra-High-Performance Concrete (UHPC) subjected to harsh ocean environment: towards an application of Layered Double Hydroxides (LDHs), Constr. Build. Mater. 177 (2018) 51–62, https://doi.org/10.1016/j.conbuildmat.2018.03.210.

[10] M. Zhou, W. Lu, J. Song, C.G. Lee, Application of ultra-high-performance concrete in bridge engineering, Constr. Build. Mater. 186 (2018) 1256–1267, https://doi.org/10.1016/j.conbuildmat.2018.08.036.

[11] U. Schneider, Concrete at high temperatures — a general review, Fire Saf. J. 13 (1988) 55–56, https://doi.org/10.1016/0379-7112(88)90033-1.

[12] X. Liang, C. Wu, Y. Yang, Z. Li, Experimental study on ultra-high performance concrete with high fire resistance under simultaneous effect of elevated temperature and impact loading, Cem. Concr. Compos. 98 (2019) 29–38, https://doi.org/10.1016/j.cemconcomp.2019.01.017.

[13] D. Ghosh, A. Abd-Elssamd, Z. Ma, D. Hun, Development of high-early-strength fibre-reinforced self-compacting concrete, Constr. Build. Mater. 266 (2021), 121051, https://doi.org/10.1016/j.conbuildmat.2020.121051.

[14] R.A. Raju, S. Lim, M. Akiyama, T. Kageyama, Effects of concrete flow on the distribution and orientation of fibres and flexural behavior of steel fibre-reinforced self-compacting concrete beams, Constr. Build. Mater. 262 (2020), 119963, https://doi.org/10.1016/j.conbuildmat.2020.119963.

[15] B. Ramesh, V. Gokulnath, M. Ranjith Kumar, Detailed study on flexural strength of polypropylene fibre reinforced self-compacting concrete, Mater. Today: Proc. 22 (2020) 1054–1058, https://doi.org/10.1016/j.matpr.2019.11.292.

[16] A. Rashno, A. Saghaeifar, Durability of ultra-high performance self-compacting concrete with hybrid fibre, Emerg. Mater. Res. 9 (2) (2020) 1–12, https://doi.org/10.1680/jemmr.19.00083.

[17] J. Sanjeev, K.J.N. Sai Nitesh, Study on the effect of steel and glass fibres on fresh and hardened properties of vibrated concrete and self-compacting concrete, Mater. Today.: Proc. 27 (2020) 1559–1568, https://doi.org/10.1016/j.matpr.2020.03.208.

[18] Zohreh Salari, B. Vakhshouri, S. Nejadi, Analytical review of the mix design of fiber reinforced high strength self-compacting concrete, J. Build. Eng. 20 (2018) 264–276, https://doi.org/10.1016/j.jobe.2018.07.025.

[19] Z. Algin, M. Ozen, The properties of chopped Basalt fibre reinforced self-compacting concrete, Constr. Build. Mater. 186 (2018) 678–685, https://doi.org/10.1016/j.conbuildmat.2018.07.089.

[20] V.J. John, B. Dharmar, Influence of Basalt fibers on the mechanical behavior of concrete—a review, Int. Fed. Struct. Concr. (2021-2022) 491–502, https://doi.org/10.1002/suco.201900086.

[21] Sa Cui, X. Xu, X. Yan, Z. Chen, C. Hu, Z. Liu, Experimental study on the interfacial bond between short cut Basalt fibre bundles and cement matrix, Constr. Build. Mater. 256 (2020), 119353, https://doi.org/10.1016/j.conbuildmat.2020.119353.

[22] H. Dilbas, Ö. Çakır, Influence of Basalt fibre on physical and mechanical properties of treated recycled aggregate concrete, Constr. Build. Mater. 254 (2020), 119216, https://doi.org/10.1016/j.conbuildmat.2020.119216.

[23] M.G. Sohail, W. Alnahhal, A. Taha, K. Abdelaal, Sustainable alternative aggregates: characterization and influence on mechanical behavior of Basalt fibre reinforced concrete, Constr. Build. Mater. 255 (2020), 119365, https://doi.org/10.1016/j.conbuildmat.2020.119365.

[24] C. Zhang, W. Wang, X. Zhang, Y. Ding, P. Xu, Mechanical properties and microstructure of Basalt fibre-reinforced recycled concrete, J. Clean. Prod. 278 (2021), 123252, https://doi.org/10.1016/j.jclepro.2020.123252.

[25] A. Alaskar, A. Albidah, A. Alqarni, R. Alyousef, H. Mohammad hosseini, Performance evaluation of high-strength concrete reinforced with Basalt fibers exposed to elevated temperatures, J. Build. Eng. 35 (2021), 102108, https://doi.org/10.1016/j.jobe.2020.102108.

[26] D. Wang, Y. Ju, X. Shen, L. Xu, Mechanical properties of high-performance concrete reinforced with Basalt fibre and polypropylene fibre, Constr. Build. Mater. 197 (2019) 464–473, https://doi.org/10.1016/j.conbuildmat.2018.11.181.

[27] J.H. Haido, A.B. Tayeh, S.S. Majeed, M. Karpuzcu, Effect of high temperature on the mechanical properties of Basalt fibre self-compacting concrete as an overlay material, Constr. Build. Mater. 268 (2020), 121725, https://doi.org/10.1016/j.conbuildmat.2020.121725.

[28] A. Saradar, P. Nemati, A.S. Paskiabi, M.M. Moein, H. Moez, E.H. Vishki, Prediction of mechanical properties of lightweight Basalt fiber reinforced concrete containing silica fume and fly ash: experimental and numerical assessment, J. Build. Eng. 32 (2020), 101732, https://doi.org/10.1016/j.jobe.2020.101732.

[29] J.G. Shao, S. Wang, Y. Liu, P. Zhang, G.B. Tang, Y.G. Jin, C.C. Li, Experimental study of basic mechanical properties of short Basalt fiber bundle reinforced concrete, J. Phys.: Conf. Ser. 2158 (2022), https://doi.org/10.1088/1742-6596/2158/1/012037.

[30] L. Xu, D. Song, N. Liu, W. Tian, Study on mechanical properties of Basalt fiber-reinforced concrete with high content of stone powder at high temperatures, Adv. Mater. Sci. Eng. (2021) 15, https://doi.org/10.1155/2021/7517049.

[31] M. Hassani Niaki, A. Fereidoon, M. Ghorbanzadeh Ahangari, Experimental study on the mechanical and thermal properties of Basalt fibre and nanoclay reinforced polymer concrete, Compos. Struct. 191 (2018) 231–238, https://doi.org/10.1016/j.compstruct.2018.02.063.

[32] W. Yonggui, L. Shuaipeng, P. Hughes, F. Yuhui, Mechanical properties and microstructure of Basalt fibre and nano-silica reinforced recycled concrete after exposure to elevated temperatures, Constr. Build. Mater. 247 (2020), 118561, https://doi.org/10.1016/j.conbuildmat.2020.118561.

[33] P. Smarzewski, Property Assessment of Self-compacting Basalt Fiber Reinforced Concrete 36, Lublin University of Technology, 2022, pp. 186–197, https://doi.org/10.1007/978-3-030-83719-8_17.

[34] N. Gupta, R. Siddique, R. Belarbi, Sustainable and greener self-compacting concrete incorporating industrial by-products: a review, J. Clean. Prod. 284 (2021), 124803, https://doi.org/10.1016/j.jclepro.2020.124803.

[35] H. Moosberg-Bustnes, B. Lagerblad, E. Forssberg, The function of filler in concrete, material and structure, Mater. Constr., vol. 37, 2004, pp. 74–81. ⟨https://doi.org/10.1007/BF02486602⟩.

[36] R. Kaminskas, I. Barauskas, R. Kubiliute, D. Monstvilaite, The effect of the pozzolanic activity of different micro-fillers on Portland cement hydration, Ceramics-Silikáty 64 (2) (2020) 145–154, https://doi.org/10.13168/cs.2020.0003.

[37] G. Rojo-Lopez, S. Nunes, B. Gonzalez-Fonteboa, F. Martinez-Abella, Quaternary blends of Portland cement, metakaolin, biomass ash and granite powder for production of self-compacting concrete, J. Clean. Prod. 266 (2020), https://doi.org/10.1016/j.jclepro.2020.

[38] Olga M. Smirnova, Low-clinker cements with low water demand, J. Mater. Civ. Eng. 32 (2020) 06020008, https://doi.org/10.1061/(ASCE)MT.1943-5533.0003241.

[39] G. Hernandez, A. Tagnit-Hamou, Optimization of ultra-high-performance concrete by use of soft and hard inert fillers (limestone and quartz), ACI Mater. J. (2022), https://doi.org/10.14359/51734222.

[40] S. Mehdipour, I.M. Nikbin, S. Dezhampanah, R. Mohebbi, H. Moghadam, S. Charkhtab, A. Moradi, Mechanical properties, durability and environmental evaluation of rubberized concrete incorporating steel fiber and metakaolin at elevated temperatures, J. Clean. Prod. 254 (2020), https://doi.org/10.1016/j.jclepro.2020.120126.

[41] M. Benaicha, X. Roguiez, O. Jalbaud, V. Yves Burtschell, A. Alaoui, Influence of silica fume and viscosity modifying agent on the mechanical and rheological behavior of self-compacting concrete, Constr. Build. Mater. 84 (2015) 103–110, https://doi.org/10.1016/j.conbuildmat.2015.03.061.

[42] H.Y. Leung, J. Kim, A. Nadeem, J. Jaganathan, M.P. Anwar, Sorptivity of self-compacting concrete containing fly ash and silica fume, Constr. Build. Mater. 113 (2016) 369–375, https://doi.org/10.1016/j.conbuildmat.2016.03.071.

[43] Yousef R. Alharbi, Aref A. Abadel, Ola A. Mayhoub, Mohamed Kohail, Effect of using available metakaolin and nano materials on the behavior of reactive powder concrete, Constr. Build. Mater. 269 (2021), 121344, https://doi.org/10.1016/j.conbuildmat.2020.121344 (ISSN 0950-0618).

[44] H.M. Ibrahim, M.A. Arab, A.M. Faisal, Feasibility of using metakaolin as a self-compacted concrete constituent material, in: Proc. of the Fourth International Conference on Advances in Civil, Structural and Environmental Engineering - ACSEE 2016, 2016. ⟨https://doi.org/10.15224/978-1-63248-114-6-25⟩.

[45] V. Kannan, K. Ganesan, Chloride and chemical resistance of self-compacting concrete containing rice husk ash and metakaolin, Constr. Build. Mater. 51 (2014) 225–234, https://doi.org/10.1016/j.conbuildmat.2013.10.050.

[46] S. Lenka, K.C. Panda, Effect of metakaolin on the properties of conventional and self-compacting concrete, Adv. Concr. Constr. 5 (1) (2017) 31–48, https://doi.org/10.12989/acc.2017.5.1.31.

[47] G. Rojo-Lopez, S. Nunes, B. Gonzalez-Fonteboa, F. Martinez-Abella, Quaternary blends of Portland cement, metakaolin, biomass ash and granite powder for production of self-compacting concrete, J. Clean. Prod. 266 (2020) 1–14, https://doi.org/10.1016/j.jclepro.2020.121666.

[48] H.E. Elyamany, A.M. Abd Elmoaty, B. Mohamed, Effect of filler types on physical, mechanical and microstructure of self-compacting concrete and flow-able concrete, Alex. Eng. J. 53 (2014) 295–307, https://doi.org/10.1016/j.aej.2014.03.010.

[49] R. Saleh Ahari, T. Erdem, K. Ramyar, Effect of various supplementary cementitious materials on rheological properties of self-consolidating concrete, Const. Build. Mater. 75 (2015) 89–98, https://doi.org/10.1016/j.conbuildmat.2014.11.014.

[50] I.P. Sfikas, E.G. Badogiannis, K.G. Trezos, Rheology and mechanical characteristics of self-compacting concrete mixtures containing metakaolin, Constr. Build. Mater. 64 (2014) 121–129, https://doi.org/10.1016/j.conbuildmat.2014.04.048.

[51] R. Madandoust, S.Y. Mousavi, Fresh and hardened properties of self-compacting concrete containing metakaolin, Constr. Build. Mater. 35 (2012) 752–763, https://doi.org/10.1016/j.conbuildmat.2012.04.109 (753).

[52] G. Chand, S. Kumar, H. Shobha, Assessment of the properties of sustainable concrete produced from quaternary blend of Portland cement, glass powder, metakaolin and silica fume, Clean. Eng. Technol. 4 (2021), 100179, https://doi.org/10.1016/j.clet.2021.100179.

[53] L.R.C. Tavares, J.F.T. Junior, L.M. Costa, A.C. d Bezerra, P.R. Cetlin, M.T.P. Aguilar, Influence of quartz powder and silica fume on the performance of Portland cement, Nat. Res. 10 (2020), https://doi.org/10.1038/s41598-020-78567-w.

[54] P. Lawrence, M. Cyr, E. Ringot, Mineral admixtures in mortars: effect of inert materials on short-term hydration, Cem. Concr. Res. 33 (12) (2003) 1939–1947, https://doi.org/10.1016/S0008-8846(03)00183-2.

[55] P. Chindaprasirt, T. Sinsiri, W. Kroehong, C. Jaturapitakkul, A.M. ASCE, Role of filler effect and pozzolanic reaction of biomass ashes on hydrated phase and pore size distribution of blended cement paste, J. Mater. Civ. Eng. (2014), https://doi.org/10.1061/(ASCE)MT.1943-5533.0000921.

[56] M.H. Lai, S.A.M. Binhowimal, L. Hanzic, Q. Wang, J.C.M. Ho, Dilatancy mitigation of cement powder paste by pozzolanic and inert Fillers, Int. Fed. Struct. Concr. (2020&;;2021) 1164–1180, https://doi.org/10.1002/suco.201900320.

[57] V. Corinaldesi, G. Moriconi, Characterization of self-compacting concretes prepared with different fibers and mineral additions, Cem. Concr. Compos., vol. 33, 201, pp. 596–601. ⟨https://doi.org/10.1016/j.cemconcomp.2011.03.007⟩.

[58] M. Mahoutian, M. Shekarchi, Effect of inert and pozzolanic materials on flow and mechanical properties of self-compacting concrete, J. Mater. (2015) 11, https://doi.org/10.1155/2015/239717.

[59] G. Ye, X. Liu, G. De Schutter, A.-M. Poppe, L. Taerwe, Influence of limestone powder used as filler in SCC on hydration and microstructure of cement pastes, Cem. Concr. Compos. 29 (2007) 94–102, https://doi.org/10.1016/j.cemconcomp.2006.09.003.

[60] J. Tikkanen, A. Cwirzen, V. Penttala, Effects of mineral powders on hydration process and hydration products in normal strength concrete, Constr. Build. Mater. 72 (2014) 7–14, https://doi.org/10.1016/j.conbuildmat.2014.08.066.

[61] L. Mello, M. Anjos, M. Sá, N. Souza, E. Farias, Effect of high temperatures on self-compacting concrete with high levels of sugarcane bagasse ash and metakaolin, Constr. Build. Mater. 248 (2020), 118715, https://doi.org/10.1016/j.conbuildmat.2020.118715.

[62] N. Abdelmelek, E. Lubloy, The impact of metakaolin, silica fume and fly ash on the temperature resistance of high strength cement paste, J. Therm. Anal. Calorim. 147 (2022) 2895–2906, https://doi.org/10.1007/s10973-021-10700-x.

[63] M. Saad, S.A. Abo-El-Enein, G.B. Hanna, M.F. Kotkata, Effect of silica fume on the phase composition and microstructure of thermally treated concrete, Cem. Concr. Res. 26 (10) (1996) 1479–1484, https://doi.org/10.1016/0008-8846(96)00142-1.

[64] M. Saad, S.A. Abo-El-Enein, G.B. Hanna, M.F. Kotkata, Effect of temperature on physical and mechanical properties of concrete containing silica fume, Cem. Concr. Res. 26 (5) (1996) 669–675, https://doi.org/10.1016/S0008-8846(96)85002-2.

[65] N. Abdelmelek, N.S. Alimrani, N. Krelias, E. Lubloy, Effect of elevated temperatures on microstructure of high strength concrete based-metakaolin, J. King Saud. Univ. (2021), https://doi.org/10.1016/j.jksues.2021.08.001.

[66] M.S. Morsy, A.M. Rashad, S.S. Shebl, Effect of elevated temperature on compressive structure of blended cement mortar, Build. Res. J. 56 (2008) 173–185.

[67] M. Uysa, Self-compacting concrete incorporating filler additives: performance at high temperatures, Constr. Build. Mater. 26 (2012) 701–706, https://doi.org/10.1016/j.conbuildmat.2011.06.077.

[68] A.M. Rashad, S.R. Zeedan, A preliminary study of blended pastes of cement and quartz powder under the effect of elevated temperature, Constr. Build. Mater. 29 (2012) 672–681, https://doi.org/10.1016/j.conbuildmat.2011.10.006.

[69] G.C. Isaia, A.L.G. Gastaldini, R. Moraes, Physical and pozzolanic action of mineral additions on the mechanical strength of high-performance concrete, Cem. Concr. Compos. 25 (2003) 69–76 (PII: S09 58-9465 (01)00057-9).

[70] P.R. Da Silva, J. De Brito, Experimental study of the porosity and microstructure of Self-Compacting Concrete (SCC) with binary and ternary mixes of fly ash and limestone filler, Constr. Build. Mater. 86 (2015) 101–112, https://doi.org/10.1016/j.conbuildmat.2015.03.110.

[71] V. Kannan, K. Ganesan, Mechanical properties of self-compacting concrete with binary and ternary cementitious blends of metakaolin and fly ash, J. South Afr. Inst. Civ. Eng. 56 (2014) 97–105. ⟨http://www.scielo.org.za/scielo.php?script=sci_abstract&pid=S1021-20192014000200011⟩.

[72] M. Gesoglu, E. Ozbay, Effects of mineral admixtures on fresh and hardened properties of self-compacting concretes: binary, ternary and quaternary systems, Mater. Struct. 40 (2007) 923–937, https://doi.org/10.1617/s11527-007-9242-0.

[73] P. Dinakar, S.N. Manu, Concrete mix design for high strength self-compacting concrete using metakaolin, Mater. Des. 60 (2014) 661–668, https://doi.org/10.1016/j.matdes.2014.03.053.

[74] Liliya Kazanskaya, Smirnova, M. Olga, Influence of mixture composition on fresh concrete workability for ballastless track slabs, E3S Web Conf. 157 (2020) 06022, https://doi.org/10.1051/e3sconf/202015706022.

[75] R. Chinthakunta, R.D. Prasad, C.M. Sri Rama, Y.M. Janardhan, Performance evaluation of self-compacting concrete containing fly ash, silica fume and nano titanium oxide, Mater. Today: Proc., vol. 43, 202, pp. 2348–54. ⟨https://doi.org/10.1016/j.matpr.2021.01.681⟩.

[76] T.V. Fonseca, M.A.S. dos Anjos, R.L.S. Ferreira, F.G. Branco, L. Pereira, Evaluation of self-compacting concretes produced with ternary and quaternary blends of different SCM and hydrated-lime, Constr. Build. Mater. 320 (2022), https://doi.org/10.1016/j.conbuildmat.2021.126235.

[77] P. Promsawat, B. Chatveer, G. Sua-iam, N. Makul, Properties of self-compacting concrete prepared with ternary portland cement-high volume fly ash-calcium carbonate blends, Case Stud. Constr. Mater. 13 (2020), https://doi.org/10.1016/j.cscm.2020.e00426.

[78] P. Danish, G.G. Mohan, Behavior of self-compacting concrete using different mineral powders additions in ternary blend, Rev. Rom. Mater./Rom. J. Mater. 50 (2020) 232–239.

[79] J. Ma, J. Dietz, Ultra-High-Performance Self Compacting Concrete, LACER No. 7, 2002. ⟨https://citeseerx.ist.psu.edu/viewdoc/download?doi=10.1.1.115.8138&rep=rep1&type=pdf⟩.

[80] A.S. El-Dieb, Mechanical, durability and microstructural characteristics of ultra-high-strength self-compacting concrete incorporating steel fibers, Mater. Des. 30 (2009) 4286–4292, https://doi.org/10.1016/j.matdes.2009.04.024.

[81] Z. Guo, T. Jiang, J. Zhang, X. Kong, C. Chen, D.E. Lehman, Mechanical and durability properties of sustainable self-compacting concrete with recycled concrete aggregate and fly ash, slag and silica fume, Constr. Build. Mater. 231 (2020), https://doi.org/10.1016/j.conbuildmat.2019.117115.

[82] R.S. Ahari, T.K. Erdem, K. Ramyar, Permeability properties of self-consolidating concrete containing various supplementary cementitious materials, Constr. Build. Mater. 79 (2015) 326–336, https://doi.org/10.1016/j.conbuildmat.2015.01.053.

[83] M. Gesoglu, E. Ozbay, Effects of mineral admixtures on fresh and hardened properties of self-compacting concretes: binary, ternary and quaternary systems, Mater. Struct. 40 (2007) 923–937, https://doi.org/10.1617/s11527-007-9242-0.

[84] R. Kumar, N. Shafiq, A. Kumar, A.A. Jhatial, Investigating EMbodied Carbon, Mechanical Properties, and Durability of High-performance Concrete Using Ternary and Quaternary Blends of Metakaolin, Nano-silica, and Fly Ash, Environ. Sci. Pollut. Res. 28 (2021), https://doi.org/10.1007/s11356-021-13918-2.

[85] S. Shrihari, M.V. Seshagiri Rao, V. Srinivasa Reddy, Evaluation of cementing efficiency in quaternary blended self-compacting concrete, Int. J. Civ. Eng. Technol. 10 (3) (2019) 83–90. ⟨http://www.iaeme.com/ijmet/issues.asp?JType=IJCIET&VType=10&IType=3⟩.

[86] M. Damma, D.P. Ravella, M.S.R. Chand, M.J. Yadav, Mechanical and durability characteristics of high-performance self compacting, concrete containing fly ash, silica fume and graphene oxide, Mater. Today: Proc. 43 (2021) 2361–2367, https://doi.org/10.1016/j.matpr.2021.01.684.

[87] M.A.S. Anjos, A. Camoes, P. Campos, G.A. Azeredo, R.L.S. Ferreira, Effect of high-volume fly ash and metakaolin with and without hydrated lime on the properties of self-compacting concrete, J. Build. Eng. 27 (2020), https://doi.org/10.1016/j.jobe.2019.100985.

[88] H.O. Shin, D.Y. Yoo, J.H. Lee, S.H. Lee, Y.S. Yoon, Optimized mix design for 180 MPa ultra-high-strength concrete, J. Mater. Res. Technol. 8 (2019) 4182–4197, https://doi.org/10.1016/j.jmrt.2019.07.027.

[89] G.S.L. Devi, C.V.S.R. Prasad, P.S. Rao, Influence of mineral admixtures on structural behavior of quaternary blended self-compacting concrete reinforced beams with addition of crimpled steel fibers, Mater. Today: Proc. (2022), https://doi.org/10.1016/j.matpr.2022.01.125.

[90] M.T. Bassuoni, M.L. Nehdi, Resistance of self-consolidating concrete to ammonium sulphate attack, Mater. Struct. 45 (2012) 977–994, https://doi.org/10.1617/s11527-011-9811-0.

[91] R. Kanagavel, K. Arunachalam, Experimental investigation on mechanical properties of hybrid fiber reinforced quaternary cement concrete, J. Eng. Fibers Fabr. 10 (2015) 139–147.

[92] ASTM C150M-22 Standard Specification for Portland Cement. ⟨https://doi.org/10.1002/jbm.b.31853⟩.

[93] ASTM C1240-20 Standard Specification for Silica Fume Used in Cementitious Mixtures. ⟨https://doi.org/10.1520/C1240-14.2⟩.

[94] ASTM C 494M-19E01 Standard Specification for Chemical Admixtures for Concrete.

[95] W. Li, Z. Huang, G. Hu, W.H. Duan, S.P. Shah, Early-age shrinkage development of ultra-high-performance concrete under heat curing treatment, Constr. Build. Mater. 131 (2017) 767–774, https://doi.org/10.1016/j.conbuildmat.2016.11.024.

[96] Y.N.S. Chan, G.F. Peng, M. Anson, Fire behavior of high-performance concrete made with silica fume at different moisture contents, ACI Mater. J. 95 (1999) 405–409.

[97] F. Shaikh, M. Taweel, Compressive strength and failure behaviour of fibre reinforced concrete at elevated temperatures, J. Adv. Concr. Constr. 3 (4) (2015) 283–293, https://doi.org/10.12989/acc.2015.3.4.283.

[98] V. Babrauskas, Temperatures in Flames and Fires, Fire Science and Technology Inc., 2006. ⟨https://doctorfire.com/temperatures-in-flames-and-fires/⟩.

[99] G.-F. Peng, W.-W. Yang, J. Zhao, Y.-F. Liu, S.-H. Bian, L.-H. Zheo, Explosive spalling and residual mechanical properties of fibre-toughened high-performance concrete subjected to high temperatures, Cem. Concr. Res. 36 (2006) 723–727, https://doi.org/10.1016/j.cemconres.2005.12.014.

[100] BS EN 12390 3:2019 Testing hardened concrete Part 3: Compressive strength of test specimens.

[101] ASTM C496/496M (2017) Standard Test Method for Splitting Tensile Strength of Cylindrical Concrete Specimens.

[102] ASTM C597 (2016) Standard Test Method for Pulse Velocity Through Concrete.

[103] ASTM C1585 (2020) Standard Test Method for Measurement of Rate of Absorption of Water by Hydraulic-Cement Concretes.

[104] ASTM C642 (2021) Standard Test Method for Density, Absorption, and Voids in Hardened Concrete.

[105] W. Zhu, J.C. Gibbs, Use of different limestone and chalk powders in self-compacting concrete, Cem. Concr. Res. 35 (2005) 1457–14621458, https://doi.org/10.1016/j.cemconres.2004.07.001.

[106] Q. Song, R. Yu, X. Wanga, S. Rao, Z. Shui, A novel self-compacting Ultra-High Performance Fibre Reinforced Concrete (SCUHPFRC) derived from compounded high-active powders, Constr. Build. Mater. 158 (2018) 883–893, https://doi.org/10.1016/j.conbuildmat.2017.10.059.

[107] C.S. Poon, L. Lam, S.C. Kou, Y.L. Wong, R. Wong, Rate of pozzolanic reaction of metakaolin in high-performance cement pastes, Cem. Concr. Res. 31 (2001) 1301–1306, https://doi.org/10.1016/S0008-8846(01)00581-6.

[108] M. Gesoglu, E. Güneyisi, M.E. Kocabag, V. Bayram, K. Mermerdas, Fresh and hardened characteristics of self-compacting concretes made with combined use of marble powder, limestone filler, and fly ash, Constr. Build. Mater. 37 (2012) 160–170, https://doi.org/10.1016/j.conbuildmat.2012.07.092.

[109] S. Wild, J.M. Khatib, A. Jones, Relative strength, pozzolanic activity and cement hydration in superplasticized metakaolin concrete, Cem. Concr. Res. 26 (1996) 1537–1544, https://doi.org/10.1016/0008-8846(96)00148-2.

[110] P.A. Claisse, H.I. Elsayad, I.G. Shaaban, Test methods for measuring fluid transfer in cover concrete, ASCE Mater. J. 11 (2) (1999) 138–143, https://doi.org/10.1061/(ASCE)0899-1561(1999)11:2(138).

[111] P.A. Claisse, H.I. Elsayad, I.G. Shaaban, Permeability and pore volume of carbonated concrete, ACI Mater. J. 96 (3) (1999) 378–381. ⟨http://www.concrete.org/Publications/ACIMaterialsJournal/ACIJournalSearch.aspx?m=details&ID=636⟩.

[112] P.A. Claisse, H.I. El Sayad, I.G. Shaaban, Absorption and sorptivity of cover concrete, J. Mater. Civ. Eng. Am. Soc. Civ. Eng. ASCE 9 (3) (1997) 105–110, https://doi.org/10.1061/(ASCE)0899-1561(1997)9:3(105).

[113] I.G. Shaaban, J.P. Rizzuto, A. El-Nemr, L. Bohan, H. Ahmed, H. Tindyebwa, Mechanical properties and air permeability of concrete containing waste tyres extracts, J. Mater. Civ. Eng. ASCE 33 (2) (2021), https://doi.org/10.1061/(ASCE)MT.1943-5533.0003588.

[114] S. Girish, N. Ajay, T. Soumya, Sorptivity as a durability index for service life prediction of self-compacting concrete, in: M.C. Narasimhan, V. George, G. Udayakumar, A. Kumar (Eds.), Trends in Civil Engineering and Challenges for Sustainability. Lecture Notes in Civil Engineering, 99, Springer, Singapore, 2021, https://doi.org/10.1007/978-981-15-6828-2_23.

[115] T.C. Ling, C.S. Poon, S.C. Kou, Influence of recycled glass content and curing conditions on the properties of self-compacting concrete after exposure to elevated temperatures, Cem. Concr. Compos. 34 (2012) 265–272, https://doi.org/10.1016/j.cemconcomp.2011.08.010.

[116] F. Arslan, A. Benli, M. Karatas, Effect of high temperature on the performance of self-compacting mortars produced with calcined kaolin and metakaolin, Constr. Build. Mater. 256 (2020) 119497, https://doi.org/10.1016/j.conbuildmat.2020.119497.

[117] M. Karatas, A. Benli, F. Arslan, The effects of kaolin and calcined kaolin on the durability and mechanical properties of self-compacting mortars subjected to high temperatures, Constr. Build. Mater. 265 (2020) 120300, https://doi.org/10.1016/j.conbuildmat.2020.120300.

[118] J. Tang, S. Wei, W. Li, S Ma, P. Ji, X. Shen, Synergistic effect of metakaolin and limestone on the hydration properties of Portland cement, Constr. Build. Mater. (2019), https://doi.org/10.1016/j.conbuildmat.2019.06.059.